Author Manuscript

Author Manuscript

Author Manuscript

Author Manuscript

HHS Public Access

Author manuscript

Biomaterials. Author manuscript; available in PMC 2021 January 01.

Published in final edited form as:

Biomaterials. 2020 January ; 227: 119558. doi:10.1016/j.biomaterials.2019.119558.

Synergistic combination treatment to break cross talk between cancer cells and bone cells to inhibit progression of bone metastasis

Sivakumar Vijayaraghavalu[a], **Yue Gao**[a], **Mohammed Tanjimur Rahman**[a], **Richard Rozic**[a], **Nima Sharifi**[b], **Ronald J. Midura**[a], **Vinod Labhasetwar**[a,*]

[a]Department of Biomedical Engineering, Lerner Research Institute, Cleveland Clinic, Cleveland, OH 44195, USA

[b]Genitourinary Malignancies Research Center, Department of Cancer Biology, Lerner Research Institute, Cleveland Clinic, Cleveland, OH 44195, USA

Abstract

Advanced-stage cancers often metastasize to bone, and is the major cause of cancer-related morbidity and mortality. Due to poor biodistribution of intravenously administered anticancer drugs within the bone, chemotherapy is not optimally effective in treating bone metastasis. Additionally, overexpression of receptor activator of nuclear factor κB ligand (RANKL) in the bone microenvironment drives the vicious, destructive cycle of progression of bone metastasis and bone resorption. We hypothesized that the combination treatment — with docetaxel (TXT), an anticancer drug encapsulated in sustained release biodegradable nanoparticles (TXT-NPs) that are designed to localize in bone marrow, and denosumab monoclonal antibody (DNmb), which binds to RANKL — could be more effective than either treatment alone. We tested our hypothesis in intraosseous prostate cancer (PC-3) cell-induced osteolytic mouse model of bone metastasis with treatments given intravenously. The results demonstrated better efficacy with TXT-NPs than with TXT-CrEL or saline control in inhibiting progression of metastasis and improving survival. TXT-NPs showed ~3-fold higher drug levels in metastasized bone tissue at 1 wk post-administration than TXT-CrEL, thus explaining their efficacy. However, the combination treatment (TXT-NPs + DNmb) given simultaneously was significantly more effective in inhibiting metastatic progression; it caused early tumor regression and improved survival, and caused no body weight loss or tumor

*Correspondence: Vinod Labhasetwar, Ph.D., Department of Biomedical Engineering/ND20, Cleveland Clinic, 9500 Euclid Ave., Cleveland, OH 44195, Phone: 216-445-9364; Fax: 216-444-9198; labhasv@ccf.org.

Author's contribution: SV: NP formulation and characterization, animal studies, imaging, data compilation, preparation of manuscript draft; **YG:** inoculation of cancer cells for tumor model; **MR:** Bone tumor drug study and analysis; **RR:** Micro-CT analysis; **NS:** guidance to study design and data review; **RM:** Micro-CT analysis and histochemical analysis of bone; and **VL:** Conceptualization, study supervision, data analysis, and manuscript preparation.

Data Statement: The manuscript includes required protocols in detail and data for reproducibility.

Publisher's Disclaimer: This is a PDF file of an unedited manuscript that has been accepted for publication. As a service to our customers we are providing this early version of the manuscript. The manuscript will undergo copyediting, typesetting, and review of the resulting proof before it is published in its final form. Please note that during the production process errors may be discovered which could affect the content, and all legal disclaimers that apply to the journal pertain.

Conflict of interest: VL is a co-inventor on a pending US patent application for the composition of nanoparticles and combination treatment. The conflict of interest is managed by the Conflict of Interest Committee of Cleveland Clinic in accordance with its conflict of interest policies.

Author Manuscript Author Manuscript Author Manuscript Author Manuscript

relapse, even when the treatment was discontinued, whereas TXT-NPs or DNmb alone treatments showed tumor relapse after an initial regression. Micro-CT analysis of the bone from the combination treatment showed no bone loss and normal bone mineral content, bone density, and bone volume fraction, whereas TXT-NPs or DNmb alone treatments showed bone loss. Confirming the above results, histochemical analysis of the bone from the combination treatment demonstrated normal bone morphology, and osteoblast and osteoclast cell activities. In conclusion, TXT-NPs and DNmb in combination, because of their complementary roles in breaking the cross talk between cancer cells and bone cells, was significantly effective in treating bone metastasis.

Graphical Abstract

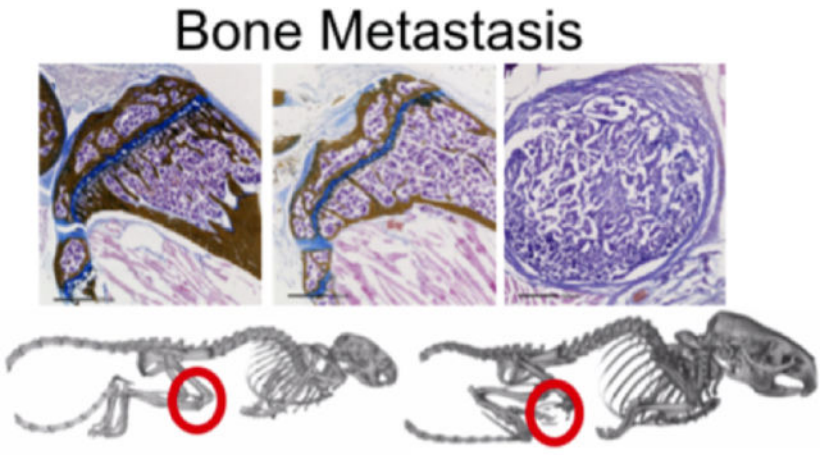

Keywords

Tumor; Drug Delivery; Nanocarriers; Biodegradable Polymers; Sustained Release; Imaging

INTRODUCTION:

Bone is a common site for metastasis in a number of human cancers because of the relatively slow blood flow through bone marrow and the presence of adhesion receptors on bone marrow capillary endothelial cells that support cancer cell localization in the bone [1, 2]. These traits, together with the bone marrow environment, which is rich in growth factors and cytokines, promote the progression of bone metastasis [3, 4]. Among cancers that metastasize to the bone, prostate and breast cancer present with significantly high incidence. About 10% of newly diagnosed prostate cancer patients present with bone metastasis, increasing to ~80% at advanced stages of the disease [5, 6]. The 5-year survival rate of patients with bone metastasis is very low compared to when the disease is localized (20% vs. 100%) [7]. Consequences of bone metastasis are often devastating; it affects bone remodeling, causes bone pain, fractures and nerve compression, and is the primary cause of prostate and breast cancer-related morbidity and mortality [8].

Since bone is less perfused (7% of cardiac output goes to bone vs. 30% to the liver) [9], intravenously administered anticancer drugs in solution do not achieve optimal levels at bone metastatic sites to inhibit tumor growth. A significant fraction of the administered drug

Author Manuscript Author Manuscript Author Manuscript Author Manuscript

is either excreted/metabolized or accumulates in other more perfused body compartments/tissue prior to reaching the marrow in sufficient doses [10]. Further, in cancer-infested bone, receptor activator of nuclear factor-κB ligand (RANKL) is involved in a vicious, destructive cyclic feedback loop between cancer cells and bone cells (osteoblasts and osteoclasts), causing bone resorption and progression of bone metastasis [11, 12]. Therefore, along with a new approach to effectively deliver anticancer drugs to the bone, a novel mechanistic approach is needed for effectively treating bone metastasis.

Previously, we have demonstrated that biodegradable nanoparticles (NPs) of specific physical properties (size and zeta potential) are effective in localizing to tumor mass in the bone marrow [10]. Further, these NPs delivering paclitaxel (PTX) following intravenous injection slowed progression of bone metastasis better than untreated control or PTX delivered using Cremophor EL (PTX-CrEL), but did not cause tumor regression [10]. In this study, we evaluated docetaxel (TXT), as it is more potent than PTX, and is also the drug of choice for treating prostate cancer [13]. Denosumab (DNmb), a monoclonal antibody, binds to RANKL and thus can downregulate osteoclast differentiation and activity [1, 14]. Hence, we hypothesized that delivery of TXT in NPs in a combination treatment with DNmb — because of their complementary roles — could effectively inhibit the progression of bone metastasis and hence bone loss. Our data demonstrated that the combination of TXT-NPs and DNmb acted synergistically to inhibit progression of bone metastasis, prevented bone loss, improved animal survival, and caused no tumor relapse even after the treatment was discontinued. Also, the animals treated with the combination showed normal bone histology and osteoclast/osteoblast cell activities.

MATERIALS AND METHODS

Materials:

Poly (D,L-lactide *co*-glycolide, 50:50; 0.69 dL/g PLGA) of inherent viscosity was purchased from LACTEL Absorbable Polymers (Birmingham, AL). Poly (vinyl alcohol) (PVA; 87–90% hydrolyzed, M.W. 30,000–70,000), (+)-Tartaric acid dimethyl ester (DMT), sodium azide, and Cremophor EL (CrEL) were purchased from Sigma-Aldrich (St. Louis, MO). Docetaxel (TXT) was obtained from Fisher Scientific (Pittsburgh, PA). Cell-culture media, Dulbecco's phosphate-buffered saline (DPBS), penicillin, and streptomycin were purchased from the Central Cell Services Media Laboratory at our institution. The CellTiter 96® AQueous One Solution Cell Proliferation Assay (MTS) was purchased from Promega (Madison, WI). All organic solvents used were of HPLC grade.

Formulation of TXT-NPs:

In a typical preparation, 80 mg PLGA, 10 mg DMT, and 10 mg TXT were dissolved in 3 mL chloroform in a glass vial by stirring at 1,000 rpm on a magnetic stir plate overnight at room temperature. The vial was wrapped with aluminum foil to protect the drug from light. DMT, a plasticizer and pore-forming agent, was used to facilitate release of the encapsulated drug from NPs [15]. The above polymer-drug solution was emulsified into 3% w/w PVA solution, first by vortexing for 1 min followed by sonication for 5 min on an ice bath using a probe sonicator at 40% (Qsonica LLC, Model Q500, Newtown, CT) to form a water-in-oil (w/o)

Author Manuscript Author Manuscript Author Manuscript Author Manuscript

emulsion. The above emulsion was stirred overnight (~18 h) at room temperature on a magnetic stir plate at 600 rpm in a fume hood set at a face velocity of 220 fpm, followed by stirring in a vacuum desiccator for 1 h to ensure removal of chloroform. The formed NPs were recovered by ultracentrifugation at 45,000 rpm (Rotor 50.2Ti, Beckman L80, Beckman Coulter, Inc., Brea, CA) at 4 °C for 45 min. The supernatant was discarded, and the pellet was re-suspended in 7 mL of MilliQ water first by vortexing and then sonicating as above for 5 min. The final dispersion was centrifuged at 4,000 rpm for 10 min at 4 °C (Sorvall Legend RT Centrifuge, Thermo Electron Corp., Waltham, MA) to remove any larger aggregates if present. The supernatant was lyophilized for 2 days at −48 °C, 3.5 Pa (FreeZone 4.5, Labconco Corp., Kansas City, MO). An identical protocol was used to formulate control NPs but without adding drug into the polymer solution. The formulation of NPs was stored at −20 °C until further use.

Physical characterization of NPs:

Mean hydrodynamic diameter and zeta potential of NPs were determined using Nicomp 380 ZLS (Particle Sizing Systems, Santa Barbara, CA). For this, the lyophilized formulation of NPs was dispersed in MilliQ water (5 mg/mL) and sonicated for 30 sec on an ice bath using a probe sonicator as above. The sample was diluted to 1:200 v/v in MilliQ water prior to sizing. The size of NPs was measured at a scattering angle of 90° at 25 °C. The undiluted sample was used to measure zeta potential in the phase-analysis mode and the current mode at a scattering angle of −14°. For transmission electron microscopy (TEM), a drop of NP-dispersion in water (~500 (μg/mL) was placed on a 200 mesh Formvar-coated TEM grid with a size of 97 μm (TED PELLA, Redding, CA). The sample was negatively stained with 2% w/v uranyl acetate solution for a min, washed with sterile MiliQ water and air dried for 3 h. The sample was imaged at 200 kV (Philips 201 TEM, Philips/FEI Inc., Briarcliff Manor, NY). The mean NP diameter was determined from 14 different images using Image J software.

TXT loading in NPs:

To 10 mg TXT-NP formulation, 5 mL methanol was added, and the sample in a closed glass vial was kept on a shaker for 48 h at 37 °C (Environ Orbital Shaker, LabLine, Melrose Park, IL). The sample was then centrifuged at 4,000 rpm for 10 min at 4 °C (Sorvall Legend RT Centrifuge, Thermo Electron Corp., Waltham, MA). The supernatant (1.5 mL) was carefully withdrawn into a 2 mL microcentrifuge tubes and centrifuged at 14,000 rpm (Eppendorf 5418 R, Hauppauge, NY) for 10 min at 4 °C; 1 mL of the supernatant was taken for HPLC analysis as described below.

TXT release from NPs:

The *in vitro* release of TXT from NPs was carried out in double diffusion chambers separated by a Millipore hydrophilic membrane of 0.05 μm porosity (VMWP01300 EMD Millipore, Burlington, MA). Each donor chamber was filled with 2.5 mL of TXT-NP suspension (1 mg/mL) in a pH 7.4 mannitol citrate buffer containing 0.1% (w/v) Tween-20 (Sigma) and 10% ethanol to maintain sink condition, and 0.1% sodium azide as a preservative. The receiver chamber was filled with buffer without NPs. Diffusion cells were covered with aluminum foil to avoid drug degradation by light and then placed on an

Author Manuscript Author Manuscript Author Manuscript Author Manuscript

Environ orbital shaker (LabLine, Melrose Park, IL) rotating at 100 rpm at 37 °C. At different time intervals, the entire content of each receiver chamber was removed and replaced with fresh buffer. The samples collected from each receiver chamber was lyophilized separately for 2 days at −48 °C, 3.5 Pa (FreeZone 4.5, Labconco Corp., Kansas City, MO). To extract drug from the lyophilized samples, 5 mL of methanol was added and kept on an orbital shaker for 48 h at 37 °C; the samples were centrifuged at 4,000 rpm for 10 min at 4 °C, and the supernatant (2 mL) was carefully drawn into an Eppendorf tube and centrifuged at 14,000 rpm for 10 min at 4 °C. The supernatant (250 μL) was collected in polypropylene micro vials with snap cap (Fisher Scientific) and quantified using HPLC-MS/MS as described below. At the end of the release study, to analyze the drug bound to diffusion chambers, they were filled with methanol and incubated at room temperature for an hour. Separately, membranes were soaked in 2 mL methanol for an hour. The methanolic-wash from the chambers and membranes were collected separately in a 2 mL Eppendorf tube and processed for quantification as described below using HPLC-MS/MS.

Analytical methods:

Drug loading in NPs was determined using HPLC (Shimadzu Scientific Instruments, Inc., Columbia, MD). The HPLC conditions were: mobile phase – methanol: acetonitrile: water (50:30:20 v/v); flow rate – 1mL/min; detector UV; wavelength – 230 nm. injection volume – 25 μL; retention time – 4.1 min. Reverse phased C18 column (Supelcosil; dimension – 25 cm × 4.6 mm; porosity 5 μm) purchased from Sigma-Aldrich. Standard plot: 0 μg to 1000 μg/mL was linear. Due to lower drug concentrations in the released samples, they were analyzed using HPLC-MS/MS. The system consisted of an HP1200 series binary pump with an online degasser, autosampler, and column heater (Agilent Technologies, Wilmington, DE). The column used was an Agilent XDB-C18 1.8 μm, 50 × 4.6 mm analytical column. The column heater was operated at 40 °C. Two eluents were used: eluent A contained water with 0.1% formic acid, and eluent B contained acetonitrile with 0.1% formic acid. A gradient was formulated as follows: 20% B to 90% B over 10 min, hold at 90% B for 5 min, and return to 20% B for 5 min. The flow rate was 500 μL/min. The mass spectrometer used was a 3200 Q TRAP® hybrid triple quadrupole/linear ion trap mass spectrometer, with a Turbo V™ ion source (SCIEX, Concord, Ontario, Canada). The source was operated in the Turbo IonSpray mode with instrument parameters including curtain gas: 10.00, ion spray voltage: 4500 V, temperature: 600 °C, nebulizer gas: 50.00, and heater gas: 50.00. The instrument's triple quadrupole mode was employed and a single MRM transition of 830.3 m/z to 304.1 m/z was collected. The declustering potential was 90 V, the collision energy was 29 V, and the dwell time was 100 msec. The integrated switching valve was configured to divert HPLC flow to waste rather than the ion source for the first 7 min to prevent unrelated compounds from fouling the ion source. A standard plot of TXT-NP in buffer (TXT dose: 0–10 μg/mL; $R^2 = 0.97$) was prepared under identical conditions.

The HPLC-MS/MS system used for tissue TXT analysis included a Vanquish UHPLC binary pump with an on-line degasser, autosampler, and column heater and a TSQ Quantiva triple quadrupole mass spectrometer with a heated electrospray (H-ESI) ion source (Thermo Fisher Scientific, Waltham, MA). The column used was an Agilent ZORBAX Eclipse XDB-C18, 4.6 × 150 mm, 5 μm analytical column (Agilent Technologies, Santa Clara, CA). Two

Author Manuscript Author Manuscript Author Manuscript Author Manuscript

eluents were used: eluent A contained water with 0.1% formic acid and eluent B contained 50:50 acetonitrile/isopropanol with 0.1% formic acid. A gradient was formulated as follows: 20%B to 90% B over 10 min, hold at 90% B for 5 min, and return to 20% B for 5 min. The flow rate was 800 μL/min. Mass spectrometer source parameters included a positive spray voltage of 3500 V, sheath gas of 60 units, aux gas of 15 units, sweep gas of 2 units, ion transfer tube temperature of 380 ºC, and vaporizer temperature of 350 ºC. Four positive ion SRM precursor/product ion pairs were collected: TXT; 808.4/105 m/z and sodium adduct of TXT. Sodium adduct which gave higher sensitivity was used for tissue drug amount calculation. Collision energies were 40 V for non-sodium adducts and 30 V for sodium adducts. The integrated switching valve was configured to divert UHPLC flow to waste rather than the ion source for the first 7 min to prevent unrelated compounds from fouling the ion source.

Cytotoxicity study in cell culture:

Androgen receptor (AR) +ve (LNCaP and C42) and -ve (PC3 and DU 145) prostate cancer cells were maintained in RPMI-1640 cell culture media supplemented with 10% fetal bovine serum (Gibco BRL, Grand Island, NY) and 100 μg/mL penicillin G and 100 μg/mL streptomycin. Cells were cultured in 100 mm cell culture dish and maintained at 37 °C in a humidified and 5% CO_2 atmosphere. After two passages, the cells were seeded into 96-well plates 24 hrs prior to drug treatments. Depending upon the protocol and cell line, seeding cell density was adjusted so that controls (untreated cells) did not become over-confluent. The cells were treated with either TXT in solution (stock; 5 mg/mL in ethanol dissolved in cell culture media) or TXT-NPs dispersed in cell culture media. First, a stock dispersion of TXT-NPs (5 mg/ml) in MilliQ water was prepared with sonication as above. The stock was diluted in cell culture medium to achieve desired concentrations. For the treatment, medium in 96-well plates was replaced with 0.1 mL medium containing drug (TXT-solution/TXT-NPs); the cells were incubated for 72 h prior to measuring cell viability using MTS assay. For experiments lasting over 5 d and 7 d post-treatment, the cells were washed at 72 h with 1xDPBS, and drug-free culture media was replaced every 48 h until the end point (5 or 7 d). For each treatment, $IC_{50/75/90}$ were calculated by non-linear curve fit (logistic) using OriginPro 8 (OriginLab Corp., Northampton, MA).

Intraosseous model of prostate cancer and treatments:

The Cleveland Clinic's Institutional Animal Care and Use Committee approved all animal procedures, and these were carried out according to Federal and internal guidelines. Athymic nude mice (nu/nu) of 5–7 weeks age were purchased from Envigo (Indianapolis, IN). Bone metastasis was induced by injecting PC-3-luc (human prostate cancer cells expressing luciferase gene; Caliper Life Sciences, Hopkinton, MA) as per our previously described protocol[1]. Briefly, 5×10^5 PC-3-luc cells were harvested from 150 cm^2 cell culture dish (Becton Dickinson Labware, Franklin Lakes, NJ) and suspended in 20 μL D-PBS. The cell suspension was then injected into the lumen of the right tibia of mice using 0.1 mL Hamilton syringe with $30_{1/2}$ gauge needle (Hamilton Company, Reno, NV). Tumor induction and its progression was monitored by measuring bioluminescence signal intensity (photons per second per square centimeter steradian; [p/s/cm^2/sr]). For bioluminescence, animals were imaged 15 min following intraperitoneal injection of luciferin (200 mg/kg;

Author Manuscript Author Manuscript Author Manuscript Author Manuscript

VivoGlo™ Luciferin, Promega, Madison, WI) using IVIS® Lumina II (PerkinElmer, Waltham, MA). To optimize the treatment schedule, animal studies were carried out in a sequential order. Based on the results, the treatments were modified to optimize therapeutic effect. All of the treatments were given intravenously via tail vein injection. In the combination treatment, both TXT-NPs and DNmb were given simultaneously. In addition to tumor growth as measured from bioluminescence signal intensity, animals were monitored for body weight and survival.

Mice were euthanized immediately if one of the following was observed: weight loss of 20%; tumor burden makes locomotion difficult; tumor ulcer; necrosis; or bleeding. Mice showing generalized signs of poor health such as dehydration, cachexia, lethargy, or hunched posture were also euthanized, and these animals were counted as dead in the survival data. A representative animal from different treatment groups was used for Micro-computed tomography (micro-CT) imaging to determine bone loss. The micro-CT data were also used to analyze bone mineral content, bone mineral density, and bone volume fraction. Additionally, the bone sections were analyzed for morphology, using histochemistry for alkaline phosphatase and tartrate-resistant acid phosphatase (TRAP) enzymatic activities.

Group I:

The purpose was to determine: a) the effect of a single dose of TXT-NPs on tumor growth regression; b) at what time point the tumor shows the relapse, and c) whether subsequent treatments are effective in regressing tumor growth. Mice were divided into two groups: treated with TXT-NPs (12 mg/kg TXT dose equivalent NPs) and saline control.

Group II:

Based on the results of Group I, the dosing frequency of TXT-NPs was modified to once in every 4 wks. The objective was also to determine: a) how effective is regular dosing on tumor regression and b) whether there is a tumor relapse after the initial regression and when the treatment was discontinued. Mice were divided into two groups: treated with TXT-NPs (12 mg/kg TXT dose) and saline control.

Group III:

The purpose was to determine: a) the effectiveness of the combination treatment on tumor regression and b) whether there is tumor relapse after the regression when the treatment is discontinued. Mice were divided into four groups: DNmb alone (3 mg/kg, as IV injection), TXT-CrEL (12 mg/kg), combination of DNmb (3 mg/kg) + TXT-NPs (12 mg/kg) given simultaneously, and saline control.

Group IV:

The purpose was to re confirm the efficacy of the combination treatment. In this group, PC-3-luc cells used for tumor inoculation were doubled (5×10^5 vs. 1×10^6) to determine the treatment response when tumor cell burden in the marrow is higher. The treatment groups included the combination of DNmb (3 mg/kg) + TXT-NPs (12 mg/kg) or TXT-NPs (12 mg/kg) and saline control.

Author Manuscript Author Manuscript Author Manuscript Author Manuscript

Micro-CT imaging and analysis to determine bone resorption:

Mice were scanned on a GE Locus RS *in vivo* Micro-CT (General Electric Company; Boston MA) equipped with a rotating gantry. Images were obtained using an X-ray tube voltage of 80 kV, a tube current of 450 μA and with exposure time of 400 ms. The detector binning was set to achieve an isotropic voxel resolution of 45 μm. Using a 1° angle of increment, 360 raw data projections were acquired. Then, 2 frames per degree were averaged for a resultant image that was later utilized for reconstruction. Reconstruction of images was performed by GE algorithms using a 16-core cluster UNIX PC.

Bone structure and mineral density metrics were evaluated using GE Microview software. For each animal, both right and left tibiae were evaluated for bone losses or gains. Post-acquisition reconstructed micro-CT volumes were calibrated using air, a solid water phantom, and a cortical bone phantom. The micro-CT volume grayscale values (correlated to Hounsfield units) were normalized to the phantom so that a standard grayscale threshold level could be applied to all volumes for bone metrics. Regions of interest were manually selected using the software splining tools for subsequent analysis and generation of global threshold-based metrics.

Bone tissue processing:

Hind limbs were recovered from euthanized mice and overlying skin was removed. The lower hind limb was isolated from the upper hind limb by sharp dissection at the knee joint. The lower hind limb was cut below the tibia/fibula synostosis using a Mar-Med Diamond Band Bone Saw (MarMed Inc., Cleveland, OH) in order to provide an opening to the medullary cavity so that fixative and other reagents would have access to the internal tissue compartments within the tibia/fibula. These samples were then fixed in neutral-buffered formalin (NBF) for 3 days at 4 °C. Samples were then transferred to ice-cold phosphate-buffered saline (PBS) to wash away excess NBF. Samples in PBS were then transferred to sterile 30% (w/v) sucrose for infiltration overnight. Samples were then positioned in a cryo-mold and frozen-embedded in OCT. Frozen tissue blocks were stored at −80 °C until cryo-sectioning. Frozen tissue blocks were cryo-sectioned at 5 microns thickness by a modification of the Dymet et al. (2016) bone cryo-sectioning procedure [16] using Kawamoto cryo-film [17]. Sections were stored flat at −20 °C until ready for staining.

Bone tissue histology:

Frozen sections were thawed and OCT/sucrose were washed away with PBS. Hydrated sections were stained using an aqueous method via a combination of von Kossa (bone), Alcian Blue (cartilage) and Nuclear Fast Red (cells and soft tissues) staining. Sections were stained with 1% silver nitrate solution under fluorescent lighting for a minimum of 6 hrs, rinsed in distilled water, exposed to 5% sodium thiosulfate for 5 min to remove un-reacted silver, rinsed in distilled water, stained in 3% Alcian blue for 30 min, rinsed in distilled water, counterstained in 0.1% Nuclear Fast Red, rinsed in distilled water and then mounted in FluorSave (EMD Millipore; #345789) mounting medium, cover-slipped and sealed with clear nail polish.

Author Manuscript Author Manuscript Author Manuscript Author Manuscript

Enzyme biomarker staining:

Frozen sections were thawed and OCT/sucrose were washed away with PBS. Hydrated sections were stained for alkaline phosphatase activity (osteoblast biomarker) using a Vecta-Red staining kit (Vector labs; SK-5100) as per manufacturer's instructions for 20 minutes at room temperature. Sections were counterstained with DAPI (1 μg/mL) for 10 min at room temperature to detect cell nuclei and then mounted in FluorSave mounting medium, cover-slipped and sealed with clear nail polish. Other frozen sections were thawed and OCT/sucrose were washed away with PBS. Hydrated sections were stained for tartrate-resistant acid phosphatase activity (osteoclast biomarker) using an ELF-97 Endogenous Phosphatase staining kit that included 5 mM levamisole as an alkaline phosphatase inhibitor (Thermo Fisher; E6601) as per manufacturer's instructions for 15 min at room temperature. Sections were counterstained with DAPI (1 μg/mL) for 10 min at room temperature to detect cell nuclei and then mounted in FluorSave mounting medium, cover-slipped and sealed with clear nail polish.

Analysis of TXT level in bone tumor tissue:

TXT-NPs or TXT-CrEL were administered via tail vein at 12 mg/kg drug equivalent dose. One week following drug administration, tumor bearing legs were resected from hip to ankle joint. Because of integration of tumor tissue with muscles and bones, it was difficult to isolate tumor tissue only. Following removal of the skin, harvested tissue were pressed on a blotting paper to remove any residual blood, weighted, chopped into small pieces, homogenized in tissue lysis buffer (Radioimmunoprecipitation assay buffer, Sigma) using tissue homogenizer (Minilys, Bertin Instruments, Bretonneux-France), lyophilized for 48 hrs. Drug from tissue was extracted in 5 mL methanol for 48 hrs at 37 °C by placing samples on an orbital shaker (100 rpm), the samples were centrifuged, first at 4,000g for 10 min at 4 °C and then aliquots of the supernatants at 16,000g for 10 min at 4 °C using a microcentrifuge. The supernatants were analyzed for TXT levels using LC-MS/MS (see details above under analytic methods). Standard plots were for TXT-NPs and TXT in methanol were used to determine tissue TXT levels. The data were normalized to per g tissue weight.

Statistical Analysis:

Data are expressed as the mean ± s.e.m. Statistical significance between untreated and treatment groups were calculated using GraphPad Prism version 7 for Windows. Tumor growth as determined from bioluminance signal intensity and body weight data were analyzed using unpaired t-test with Welch's correction. Animal survival data was plotted using Kaplan-Meier method, and statistical significance was determined using Log-rank (Mantel-Cox) test. Differences were considered significant for $p < 0.05$.

RESULTS

Physical characteristics of NPs:

The mean hydrodynamic diameter of drug-loaded NPs was 252 ± 21 nm (Figure 1a) with polydispersity index of 0.07 ± 0.02 and zeta potential of −0.6 ± 0.2 mV (n=7). The

Author Manuscript Author Manuscript Author Manuscript Author Manuscript

polydispersity index <0.1 indicates uniform size distribution of NPs. The mean TEM diameter of drug-loaded NPs was 60 ± 2.1 nm (n=200) (Figure 1b). Control NPs (without drug) were also of similar properties as drug-loaded NPs (mean hydrodynamic diameter of 314 ± 2.5, polydispersity index = 0.09 ± 0.02, zeta potential = −0.33 ± 0.2 mV, n=4). The TXT loading in NPs was 9.5 ± 0.13% w/w with an encapsulation efficiency of 94.7 ± 1.4% (n=7). The drug release followed an initial burst phase, with 30% cumulative release occurring in 1 day, 60% cumulative release in 3 days, and 75% in 8 days, with insignificant release thereafter (Figure 1c). When analyzed at the end of the release study, 5.6% of the drug remained in the donor chambers and ~0.4% remained bound to the membranes and donor/receiver chambers after they were emptied and rinsed. Thus, there is about ~18% of the drug that was not accountable, which appears to be the fraction that has degraded during the release study. The HPLC analysis of the released samples, particularly those collected at later time points, showed additional peaks; these peaks, when combined with drug peaks, showed the cumulative drug release to be almost 100%.

Cytotoxicity with TXT-NPs:

In general, TXT-NPs required a higher equivalent drug dose than TXT-solution to achieve the same level of cytotoxicity, although this difference was minimal in AR -ve PC-3 and DU145 cells compared with AR +ve LNCaP and C42 cells. Cytotoxicity was also cell-line dependent, with AR −ve cells showing better sensitivity to the treatment than AR +ve cells (Table 1). Since NPs are a sustained release formulation, the dose required to achieve the same level of cytotoxicity as compared to the drug solution is anticipated to be higher. Control NPs had no effect on cell cytotoxicity and followed the same growth curve as that of the cells grown in culture medium without any treatment.

Efficacy of treatments in bone metastasis model:

Following confirmation of tumor induction from the bioluminance signal, animals received the first intravenous dose of treatment at ~1 wk post-tumor inoculation. The purpose of the Group I experiments was to determine at what time point tumor begins to regrow after receiving the first dose of TXT-NPs, and whether the subsequent treatments are effective in suppressing tumor growth. The data show that tumor begins to grow at 8 wks after receiving the first dose of TXT-NPs. The subsequent treatment with TXT-NP at 8 wks suppressed the tumor growth, but it began to re-grow at 12 wks. The treatment at 14 wks with TXT-NP was not significantly effective in suppressing tumor growth (Figure 2a). The animals in the treatment groups gained weight until 8 wks, but not thereafter (Figure 2b). All the animals in the saline group died at 12 wks; however, no mortality was seen in the treated group until 12 wks, but it reached 60% by 20 wks (Figure 2c). The animals that survived until the end of the study also showed high tumor burden (Figure 2c).

The results of the Group I study suggested that the effect of PTX-NPs lasts for ~5–6 wks, as tumor begins to regrow thereafter and the subsequent treatments are less effective. Therefore, we reasoned that the treatment at an interval of 4 wks, which is just before tumor begins to regrow, could be more effective than after the tumor regrowth. Therefore, the animals in Group II received TXT-NPs dosing once every 4 wks. Based on the bioluminance signal, these animals showed almost complete tumor regression after receiving the last dose

Author Manuscript Author Manuscript Author Manuscript Author Manuscript

at 21 wks, but tumor relapse occurred at 42 wks. Animals in the treatment group gained weight until 21 wks, but showed weight loss thereafter. Overall, the survival of treated animals was 60% until 44 wks, whereas all the animals in saline control died at 16 wks (Figure 3).

The results of the Group II study showed overall better outcome in terms of tumor growth inhibition and survival as compared with the results of Group I study; however, tumor relapsed occurred after a gap of ~20 wks since receiving the last dose at 21 wks (Figure 3a). Also, after receiving the last dose at 21 wks, animals showed body weight loss (Figure 3b), and mortality increased although the tumor burden during 21–37 wks was significantly low (Figure 3c). Compared with saline control, the treatment with TXT-NPs every 4 wks was effective in regressing tumor growth and improving survival (100% mortality in the saline control vs. no mortality in the TXT-NP-treated group at 16 wks); however, weight loss and increased mortality beyond 21 wks could potentially be due to drug toxicity with a total of 6 doses of the treatment (Figure 3b and c). The animals that survived until the end of the study also showed high tumor burden.

In the Group III study, the combination treatment (TXT-NPs + DNmb) was tested along with other treatments for comparison, and the total treatment doses were reduced from 6 used in Group II study to 4 given once every four weeks. The data show that the combination treatment was most effective in suppressing tumor growth even after receiving the first dose of treatment. DNmb-alone treatment caused tumor growth suppression after four doses but showed tumor relapse at 36 wks. The combination treatment did not show tumor relapse even when the treatment was discontinued after the last (4^{th}) dose at the13^{th} week. The animals treated with TXT-CrEL showed early mortality (100% animal death at 11 wks), which was slightly better than saline control (100% animal death at 7 wks). DNmb-alone-treated animals exhibited tumor growth suppression and gained weight but showed tumor relapse and 60% mortality by 40 wks (Figure 4).

To reconfirm the efficacy of combination treatment, the Group IV animals received the same combination treatment as in Group-III, but included TXT-NPs treatment for comparison (which was not included in Group III but was used in Group II). The number of cells used for tumor induction was double that used in previous experiments. In this repeat study, the combination treatment showed a similar outcome in terms of tumor growth inhibition, body weight gain, and survival as in Group III. Treatment with TXT-NPs was also effective, but as shown in the Group II study, it showed tumor relapse once the treatment was discontinued (Figure 5).

In brief, the above animal data from different treatment groups demonstrated better efficacy of the treatment with TXT-NPs than with TXT-CrEL in reducing toxicity (based on weight loss) and improving survival. The combination treatment (TXT-NPs + DNmb) was significantly more effective in inhibiting metastatic progression, maintaining weight gain, and improving animal survival. The combination treatment caused early tumor regression, whereas TXT-NPs or DNmb alone-treatments required multiple dosing to achieve tumor regression. Further, there was no tumor relapse with the combination treatment even when it

Author Manuscript Author Manuscript Author Manuscript Author Manuscript

was discontinued, whereas TXT-NPs or DNmb-alone treatments showed tumor relapse after an initial regression.

The micro-CT analysis at 9 wks showed bone loss in the untreated control but not in the TXT-NP-treated animal. However, at 25 wks, the TXT-NP-treated animal showed signs of bone loss, but not the animals treated with the combination (TXT-NPs + DNmb). The animals treated with DNmb alone showed bone loss at both early (9 wks) and late (40 wks) stages when there is a tumor replace (Figure 6). Further, the animals treated with the combination demonstrated similar bone mineral content, bone density, and bone volume fraction as that of the contralateral bone or the bone of the control animal that was not inoculated with tumor cells (Table 2).

The histochemical analyses of the bone of the combination treated-animal demonstrated normal bone morphology and alkaline phosphate activity (a marker for osteoblasts) and tartrate-resistant acid phosphatase (TRAP) activity (a marker for osteoclasts) (Figure 7).

TXT levels in bone tumor tissue:

The results show ~3-fold greater drug levels in metastasized bone tissue in animals treated with TXT-NPs than with TXT-CrEL at one-week post-administration (Figure 8).

DISCUSSION:

Bone metastases occur in more than 1.5 million patients with cancer worldwide. Without an effective treatment, metastasis remains a major cause of morbidity and mortality. Our results in an animal model of bone metastasis show that the combination treatment with TXT-NPs and DNmb, given simultaneously once every four weeks for a total of four injections, was effective in regressing tumor growth, thus preventing bone loss and improving survival. The important finding was that the combination treatment did not cause tumor relapse even when the treatment was discontinued, and retained normal bone morphology and bone cell activities.

The efficacy of the combination treatment can be attributed to the formulation characteristics of TXT-NPs and the mechanistic rationale for delivering these NPs in combination with DNmb. Previously, we have demonstrated that the NPs with neutral zeta potential are more effective in localizing to bone marrow than the NPs with anionic or cationic zeta potential [10]. This is because neutral NPs have reduced interactions with serum proteins and hence are not opsonized to the same extent as cationic or anionic NPs [18]; therefore, neutral NPs remain in circulation longer and can extravasate through the fenestration in the bone marrow. The NP size also played a critical role since the openings in bone fenestrations are typically 170 nm [19, 20]. Although the mean hydrodynamic diameter of our NPs is larger than the opening in fenestrations, there is a major fraction of TXT-NPs that is lower than 170 nm (Figure 1a). However, the TEM diameter (60 nm), which is measured in a dry state, is significantly below the opening in the bone marrow fenestrations (Figure 1b). The hydrodynamic diameter is measured in a hydrated state which, in this case, includes hydration of the PVA associated with NP surface that can significantly add to the hydrodynamic diameter of NPs [21]. We have previously reported the discrepancy between

Author Manuscript Author Manuscript Author Manuscript Author Manuscript

the TEM and hydrodynamic diameters of PLGA-NPs formulated using PVA as an emulsifier [22].

Nonetheless, the efficacy of the TXT-NPs is evident, as they show better effect on tumor regression and improved survival, and less body weight loss than saline control animals (Figures 2 and 3) or those treated with TXT-CrEL (Figure 4). This is also evident from the significantly greater median survival time for TXT-NPs vs. saline or TXT-Cr-EL-treated animals (saline group = 9.5 wks, TXT-CrEL = 9 wks, TXT-NPs > 48 wks). The results show that TXT-CrEL treatment has no effect on median survival time as compared with saline control animals. Despite better outcomes with the TXT-NPs than with saline or TXT-CrEL-treated animals, our data show that the treatment with TXT-NPs needs to be given at regular intervals; otherwise, the tumor progresses (Figure 2 vs. Figure 3) and then becomes non-responsive to the treatment, suggesting that cancer cells may have developed drug resistance. However, even with a regular dosing of TXT-NPs, the tumor progressed once the treatment was discontinued (Figure 3a). The results of these studies suggest that continued dosing of TXT-NPs may be needed even after the tumor has regressed in order to minimize the risk of residual tumor cells causing relapse and becoming more aggressive. Hence, a better option would be to develop a treatment that does not cause tumor relapse even if the treatment is discontinued.

RANKL is known to promote invasiveness of cancers that metastasize to bone [23]; hence the blockage of RANKL activity has been suggested as a potential therapeutic strategy for interfering in tumor metastasis and progression to bone [24]. DNmb is a monoclonal antibody that blocks the RANKL by binding to its receptor RANK on osteoclasts, resulting in reduced bone resorption and thus less release of growth factors required for tumor growth [25]. Our data show that DNmb alone-treatment required multiple dosing to achieve tumor regression but eventually showed tumor relapse, more bone loss, and mortality by 30–40 wks (Figure 4). The micro-CT data show bone loss in few DNmb alone-treated animals even at early time points (9 wks), thus explaining the mortality, whereas the TXT-NP alone-treated animals did not show such bone loss at early time points (Figure 6). Based on the median survival, TXT-NPs alone-treatment provides better outcome than DNmb alone-treatment (14 wks vs. > 48 wks). However, DNmb alone-treatment shows better survival than saline control or TXT-CrEL treatment (40% survival by 40 wks for DNmb vs. 0% by <16 wks for saline control or TXT-CrEL).

The combination treatment (TXT-NPs + DNmb) seems to address the issues associated with TXT-NP and DNmb alone-treatments, as it showed no tumor relapse even when the treatment was discontinued (Figure 4) or bone loss (Figure 6). Although we have previously shown that the similarly formulated NPs extravasate into the bone marrow and co-localize with the tumor mass in the marrow [10], our current data show ~3-fold higher drug levels in the metastasized bone in animals treated with TXT-NPs than those treated with TXT-CrEL (Fig 8). TXT as such has a short first half-life (~17 hrs) but prolonged terminal half-life (~86 hrs) [26] but like other anticancer drugs, TXT biodistribution is mostly to vascular organs that have with high cardiac output such as to the liver, kidney, and intestine [27]. On the other hand, TXT-NPs can provide sustained drug effect (Figure 1c), thus explaining the differences in drug levels in metastasized bone tissue (Figure 8) and efficacy seen with TXT-

Author Manuscript Author Manuscript Author Manuscript Author Manuscript

NP and TXT-CrEL treated animals. Further pharmacokinetic and biodistribution study and histological analysis of vital organs along with changes in blood parameter would explain reduced toxicity of TXT-NPs over TXT-CrEL.

The efficacy of the combination treatment could be attributed to sustained and localized delivery of TXT to tumor tissue in bone marrow with NPs and DNmb playing a synergistic role in breaking the cross talk between cancer cells and bone cells (Figure 9). Importantly, the combination treatment has been seen to retain normal bone morphology (Figure 7A) and bone cell activities (osteoblast and osteoclast) (Figure 7B and C). Alkaline phosphatase activity is important for the mineralization of bone and represents a useful biochemical marker of bone formation. TRAP is highly expressed in osteoclasts; they play a pivotal role in bone homeostasis but are activated by metastatic tumors that then leads to bone destruction [28]. Our results show similar TRAP activity in the bone of the combination-treated animals as in the bones of normal animals (Figure 7B), suggesting that the combination treatment was effective in controlling RANKL activity as well as proliferation of cancer cells, ultimately leading to early tumor regression (Figures 4 and 5). As a result, the combination-treated animals do not show bone loss (Figure 6) and exhibit significantly better survival than DNmb or TXT-NP alone-treated animals. We also determined the combination treatment is effective even when the tumor burden is higher in bone marrow (Figure 5).

Currently, patients with bone metastasis are treated with bisphosphonates to reduce the risk of skeleton-related events and to ameliorate bone pain, as bisphosphonates can inhibit bone resorption [29]. Some studies have also reported that high doses of bisphosphonates indirectly slow the progression of bone metastasis [30] by inhibiting osteoclast-mediated bone resorption and thereby the release of growth factors necessary to promote cancer cell growth and differentiation, and subsequent tumor formation in bone [31]. However, a recent review of the data from different clinical studies showed no statistically significant improvement in survival of bisphosphonate-treated patients [32]. Furthermore, bisphosphonates show dose-limiting toxicities; at high doses and with chronic use, they cause osteonecrosis of the jaws (considered to be a consequence of their effect on circulating endothelial progenitor cells), and interfere with the normal process of angiogenesis and vasculogenesis required to maintain healthy tissue [33]. The chronic high doses of bisphosphonates completely shut off all bone remodeling, leading to a cessation of bone repair and rejuvenation of the skeleton. Over a long period of time, this allows the accumulation of dysfunctional and defective bone tissue that normally would have been removed and replaced with new bone. Radiation treatment is used mostly as a palliative therapy to relieve bone pain or to prevent morbidity due to pathologic fracture and spinal cord compression. However, radiation treatment can also destroy the bone cells, preventing bone tissue formation [34].

The other approaches such as conjugating anticancer drugs [35] or drug-loaded NPs to bone-seeking agents, e.g., bisphosphonates [36], tetracycline [37], or E-selectin (overexpressed in bone marrow endothelium) [38] have been investigated, but these remain inefficient. For example, Swami *et al.* [39] found no significant difference in the efficacy (bone loss, tumor burden, and survival) of alendronate (bisphosphonate)-conjugated, bortezomib-loaded NPs

Author Manuscript Author Manuscript Author Manuscript Author Manuscript

compared with unconjugated NPs or drug alone in a bone metastasis model of myeloma. The advantage of our TXT-NP formulation is that it does not involve any conjugation chemistry or ligand, but rather, simple modulation of their physical characteristics. A simple method of formulating drug-loaded NPs is important for clinical translation of the treatment.

We administered TXT-NPs for sustained drug effect, but DNmb was given as a solution along with TXT-NPs as an intravenous injection. Considering its long half-life even when given as an IV injection (range of 8–37 days, depending upon the dose of 0.03 to 3 mg/kg; dose used in this study = 3 mg/kg) [40], DNmb would diffuse into bone marrow to provide its sustained therapeutic effect. DNmb for human use is usually given subcutaneously (half-life = 25.4 days) once every 4 weeks for bone metastases. It has been shown to minimize bone loss associated with certain cancers; however, its effect is suboptimal in inhibiting cancer progression, and it is also associated with certain side effects, particularly hypocalcemia and higher risk of serious infections with chronic treatment [41]. As our data show, DNmb alone-treatment is well tolerated but shows tumor relapse, bone loss, and increasing animal mortality with time (Figure 4). As a further development, DNmb can be encapsulated in NPs along with TXT or as a separate formulation for its sustained localized effect in bone marrow, which can potentially reduce its dose and improve therapeutic efficacy.

In this study, we used PC-3 cells to induce a tumor that has osteolytic effect on the bone, but prostate cancer is most often osteoblastic, depending upon the cancer cell line. However, our data in different prostate cancer cell lines *in vitro* show the efficacy of TXT-NPs (Table 1), and hence our combination treatment could be effective in different types of prostate cancers that have metastasized to bone marrow.

Considering the limitations of the current approaches in treating bone metastasis, our combination treatment has significant potential. It has an immediate impact on suppressing the tumor growth, and would require dosing at a certain time interval until the tumor is eliminated from the bone marrow so that there is no risk of tumor relapse (Figure 4). The combination treatment was also seen as safe and effective, as there is no weight loss or bone loss, and maintained normal bone cell activities (Figures 6 and 7). With the appropriate drug for a particular cancer, the combination approach could potentially be explored for treating other cancers that metastasize to bone marrow, as RANKL plays a role in promoting cancer progression and invasiveness in bone marrow in different types of cancers. The polymer used in the formulations of TXT-NPs is biodegradable and FDA approved [42]. Its biodegradation properties as well as biocompatibility has been well-established [43]. Further, DNmb is clinically used for bone-related conditions. Hence, the clinical translation of the combination is highly feasible.

Conclusions:

The combination treatment of TXT-NPs and DNmb was synergistic in effectively suppressing prostate cancer tumor growth, preventing bone loss, and improving survival rate. The combination treatment also shows no toxicity, as evident from weight gain and no tumor relapse when the treatment was discontinued, and maintained normal bone morphology and bone cell activities. Thus, the simultaneous combination treatment that is given

Author Manuscript Author Manuscript Author Manuscript Author Manuscript

intravenously at a regular time interval over a certain period of time could provide a promising approach to treating advanced-stage prostate cancer, and potentially other cancers that have metastasized to bone marrow.

Supplementary Material

Refer to Web version on PubMed Central for supplementary material.

Acknowledgments:

This study was supported by a grant (1 R01 CA206189–01 to VL) from the National Cancer Institute of the National Institutes of Health.

Abbreviations

CrEL	Cremophor EL
DNmb	Denosumab monoclonal antibody
HPLC	High-performance liquid chromatography
LC-MS	Liquid chromatography-mass spectrometry
micro-CT	Micro-computed tomography
NPs	Nanoparticles
M.W.	Molecular Weight
PLGA	D,L-lactide *co*-glycolide
PVA	Poly (vinyl alcohol)
RANKL	Receptor activator of nuclear factor κB ligand
TXT	Docetaxel

References:

[1]. Dionisio MR, Mansinho A, Abreu C, Cavaco-Silva J, Casimiro S, Costa L, Clinical and translational pharmacology of drugs for the prevention and treatment of bone metastases and cancer-induced bone loss, Br J Clin Pharmacol, (2019).

[2]. Fornetti J, Welm AL, Stewart SA, Understanding the Bone in Cancer Metastasis, J Bone Miner Res, 33 (2018) 2099–2113. [PubMed: 30476357]

[3]. Coleman RE, Metastatic bone disease: clinical features, pathophysiology and treatment strategies, Cancer Treat Rev, 27 (2001) 165–176. [PubMed: 11417967]

[4]. Morrissey C, Vessella RL, The role of tumor microenvironment in prostate cancer bone metastasis, J Cell Biochem, 101 (2007) 873–886. [PubMed: 17387734]

[5]. Bubendorf L, Schöpfer A, Wagner U, Sauter G, Moch H, Willi N, Gasser TC, Mihatsch MJ, Metastatic patterns of prostate cancer: an autopsy study of 1,589 patients, Hum. Pathol, 31 (2000) 578–583. [PubMed: 10836297]

[6]. Berruti A, Dogliotti L, Bitossi R, Fasolis G, Gorzegno G, Bellina M, Torta M, Porpiglia F, Fontana D, Angeli A, Incidence of skeletal complications in patients with bone metastatic prostate cancer

Author Manuscript Author Manuscript Author Manuscript Author Manuscript

and hormone refractory disease: predictive role of bone resorption and formation markers evaluated at baseline, J. Urol, 164 (2000) 1248–1253. [PubMed: 10992374]

[7]. Tsuzuki S, Park SH, Eber MR, Peters CM, Shiozawa Y, Skeletal complications in cancer patients with bone metastases, Int J Urol, 23 (2016) 825–832. [PubMed: 27488133]

[8]. Berruti A, Dogliotti L, Bitossi R, Fasolis G, Gorzegno G, Bellina M, Torta M, Porpiglia F, Fontana D, Angeli A, Incidence of skeletal complications in patients with bone metastatic prostate cancer and hormone refractory disease: Predictive role of bone resorption and formation markers evaluated at baseline, J Urol, 164 (2000) 1248–1253. [PubMed: 10992374]

[9]. Chaudhari K. Ramanlal, Kumar A, Khandelwal V.K. Megraj, Ukawala M, Manjappa AS, Mishra AK, Monkkonen J, Murthy R.S. Ramachandra, Bone metastasis targeting: a novel approach to reach bone using Zoledronate anchored PLGA nanoparticle as carrier system loaded with Docetaxel, J Control Release, 158 (2012) 470–478. [PubMed: 22146683]

[10]. Adjei IM, Sharma B, Peetla C, Labhasetwar V, Inhibition of bone loss with surface-modulated, drug-loaded nanoparticles in an intraosseous model of prostate cancer, J Control Release, 232 (2016) 83–92. [PubMed: 27090164]

[11]. Body JJ, Casimiro S, Costa L, Targeting bone metastases in prostate cancer: improving clinical outcome, Nat Rev Urol, 12 (2015) 340–356. [PubMed: 26119830]

[12]. Weilbaecher KN, Guise TA, McCauley LK, Cancer to bone: a fatal attraction, Nat Rev Cancer, 11 (2011) 411–425. [PubMed: 21593787]

[13]. Ganju A, Yallapu MM, Khan S, Behrman SW, Chauhan SC, Jaggi M, Nanoways to overcome docetaxel resistance in prostate cancer, Drug Resist Updat, 17 (2014) 13–23. [PubMed: 24853766]

[14]. Hegemann M, Bedke J, Stenzl A, Todenhofer T, Denosumab treatment in the management of patients with advanced prostate cancer: clinical evidence and experience, Ther Adv Urol, 9 (2017) 81–88. [PubMed: 28392837]

[15]. Reddy MK, Labhasetwar V, Nanoparticle-mediated delivery of superoxide dismutase to the brain: an effective strategy to reduce ischemia-reperfusion injury, FASEB J, 23 (2009) 1384–1395. [PubMed: 19124559]

[16]. Dyment NA, Jiang X, Chen L, Hong SH, Adams DJ, Ackert-Bicknell C, Shin DG, Rowe DW, High-Throughput, Multi-Image Cryohistology of Mineralized Tissues, J Vis Exp, (2016).

[17]. Kawamoto T, Use of a new adhesive film for the preparation of multi-purpose fresh-frozen sections from hard tissues, whole-animals, insects and plants, Arch Histol Cytol, 66 (2003) 123–143. [PubMed: 12846553]

[18]. Arvizo RR, Miranda OR, Moyano DF, Walden CA, Giri K, Bhattacharya R, Robertson JD, Rotello VM, Reid JM, Mukherjee P, Modulating pharmacokinetics, tumor uptake and biodistribution by engineered nanoparticles, PLoS ONE, 6 (2011) e24374. [PubMed: 21931696]

[19]. Sarin H, Physiologic upper limits of pore size of different blood capillary types and another perspective on the dual pore theory of microvascular permeability, J Angiogenes Res, 2 (2010) 14. [PubMed: 20701757]

[20]. Taichman RS, Blood and bone: two tissues whose fates are intertwined to create the hematopoietic stem-cell niche, Blood, 105 (2005) 2631–2639. [PubMed: 15585658]

[21]. Sahoo SK, Panyam J, Prabha S, Labhasetwar V, Residual polyvinyl alcohol associated with poly (D,L-lactide-co-glycolide) nanoparticles affects their physical properties and cellular uptake, J Control Release, 82 (2002) 105–114. [PubMed: 12106981]

[22]. Prabha S, Zhou WZ, Panyam J, Labhasetwar V, Size-dependency of nanoparticle-mediated gene transfection: studies with fractionated nanoparticles, Int J Pharm, 244 (2002) 105–115. [PubMed: 12204570]

[23]. Ibrahim T, Ricci M, Scarpi E, Bongiovanni A, Ricci R, Riva N, Liverani C, De Vita A, La Manna F, Oboldi D, Serra P, Foca F, Cecconetto L, Amadori D, Mercatali L, RANKL: A promising circulating marker for bone metastasis response, Oncol Lett, 12 (2016) 2970–2975. [PubMed: 27698885]

[24]. Yuasa T, Yamamoto S, Urakami S, Fukui I, Yonese J, Denosumab: a new option in the treatment of bone metastases from urological cancers, Onco Targets Ther, 5 (2012) 221–229. [PubMed: 23055747]

Author Manuscript Author Manuscript Author Manuscript Author Manuscript

[25]. de Groot AF, Appelman-Dijkstra NM, van der Burg SH, Kroep JR, The anti-tumor effect of RANKL inhibition in malignant solid tumors - A systematic review, Cancer Treat Rev, 62 (2018) 18–28. [PubMed: 29154022]

[26]. Baker SD, Zhao M, Lee CK, Verweij J, Zabelina Y, Brahmer JR, Wolff AC, Sparreboom A, Carducci MA, Comparative pharmacokinetics of weekly and every-three-weeks docetaxel, Clin Cancer Res, 10 (2004) 1976–1983. [PubMed: 15041715]

[27]. Bradshaw-Pierce EL, Eckhardt SG, Gustafson DL, A physiologically based pharmacokinetic model of docetaxel disposition: from mouse to man, Clin Cancer Res, 13 (2007) 2768–2776. [PubMed: 17473210]

[28]. Miyamoto T, Suda T, Differentiation and function of osteoclasts, Keio J Med, 52 (2003) 1–7. [PubMed: 12713016]

[29]. Talreja DB, Importance of antiresorptive therapies for patients with bone metastases from solid tumors, Cancer Manag Res, 4 (2012) 287–297. [PubMed: 23049278]

[30]. Boissier S, Ferreras M, Peyruchaud O, Magnetto S, Ebetino FH, Colombel M, Delmas P, Delaisse JM, Clezardin P, Bisphosphonates inhibit breast and prostate carcinoma cell invasion, an early event in the formation of bone metastases, Cancer Res, 60 (2000) 2949–2954. [PubMed: 10850442]

[31]. Green JR, Clezardin P, Mechanisms of bisphosphonate effects on osteoclasts, tumor cell growth, and metastasis, Am J Clin Oncol, 25 (2002) S3–9. [PubMed: 12562045]

[32]. Lopez-Olivo MA, Shah NA, Pratt G, Risser JM, Symanski E, Suarez-Almazor ME, Bisphosphonates in the treatment of patients with lung cancer and metastatic bone disease: a systematic review and meta-analysis, Supportive Care Cancer, 20 (2012) 2985–2998.

[33]. Allegra A, Alonci A, Penna G, Granata A, Siniscalchi E. Nastro, Oteri G, Loddo S, Teti D, Cicciu D, De Ponte FS, Musolino C, Bisphosphonates induce apoptosis of circulating endothelial cells in multiple myeloma patients and in subjects with bisphosphonate-induced osteonecrosis of the jaws, Acta Haematol, 124 (2010) 79–85. [PubMed: 20639624]

[34]. Thavarajah N, Zhang L, Wong K, Bedard G, Wong E, Tsao M, Danjoux C, Barnes E, Sahgal A, Dennis K, Holden L, Lauzon N, Chow E, Patterns of practice in the prescription of palliative radiotherapy for the treatment of bone metastases at the Rapid Response Radiotherapy Program between 2005 and 2012, Curr Oncol, 20 (2013) e396–405. [PubMed: 24155637]

[35]. El-Mabhouh AA, Nation PN, Abele JT, Riauka T, Postema E, McEwan AJB, Mercer JR, A conjugate of gemcitabine with bisphosphonate (Gem/BP) shows potential as a targeted bone-specific therapeutic agent in an animal model of human breast cancer bone metastases, Oncol Res, 19 (2011) 287–295. [PubMed: 21776824]

[36]. Thamake SI, Raut SL, Gryczynski Z, Ranjan AP, Vishwanatha JK, Alendronate coated poly-lactic-co-glycolic acid (PLGA) nanoparticles for active targeting of metastatic breast cancer, Biomaterials, 33 (2012) 7164–7173. [PubMed: 22795543]

[37]. Hirabayashi H, Fujisaki J, Bone-specific drug delivery systems: approaches via chemical modification of bone-seeking agents, Clin Pharmacokinet, 42 (2003) 1319–1330. [PubMed: 14674786]

[38]. Mann AP, Tanaka T, Somasunderam A, Liu X, Gorenstein DG, Ferrari M, E-selectin-targeted porous silicon particle for nanoparticle delivery to the bone marrow, Adv Mater, 23 (2011) H278–282. [PubMed: 21833996]

[39]. Swami A, Reagan MR, Basto P, Mishima Y, Kamaly N, Glavey S, Zhang S, Moschetta M, Seevaratnam D, Zhang Y, Liu J, Memarzadeh M, Wu J, Manier S, Shi J, Bertrand N, Lu ZN, Nagano K, Baron R, Sacco A, Roccaro AM, Farokhzad OC, Ghobrial IM, Engineered nanomedicine for myeloma and bone microenvironment targeting, Proc Natl Acad Sci U S A, 111 (2014) 10287–10292. [PubMed: 24982170]

[40]. Amgen Australia Pty Ltd, Australian Public Assessment Report for Denosumab, https://www.tga.gov.au/sites/default/files/auspar-prolia.pdf, (2011).

[41]. Gul G, Sendur MA, Aksoy S, Sever AR, Altundag K, A comprehensive review of denosumab for bone metastasis in patients with solid tumors, Curr Med Res Opin, 32 (2016) 133–145. [PubMed: 26451465]

Author Manuscript Author Manuscript Author Manuscript Author Manuscript

[42]. Panyam J, Labhasetwar V, Biodegradable nanoparticles for drug and gene delivery to cells and tissue, Adv Drug Deliv Rev, 55 (2003) 329–347. [PubMed: 12628320]

[43]. Panyam J, Dali MM, Sahoo SK, Ma W, Chakravarthi SS, Amidon GL, Levy RJ, Labhasetwar V, Polymer degradation and in vitro release of a model protein from poly(D,L-lactide-co-glycolide) nano- and microparticles, J Control Release, 92 (2003) 173–187. [PubMed: 14499195]

Author Manuscript Author Manuscript Author Manuscript Author Manuscript

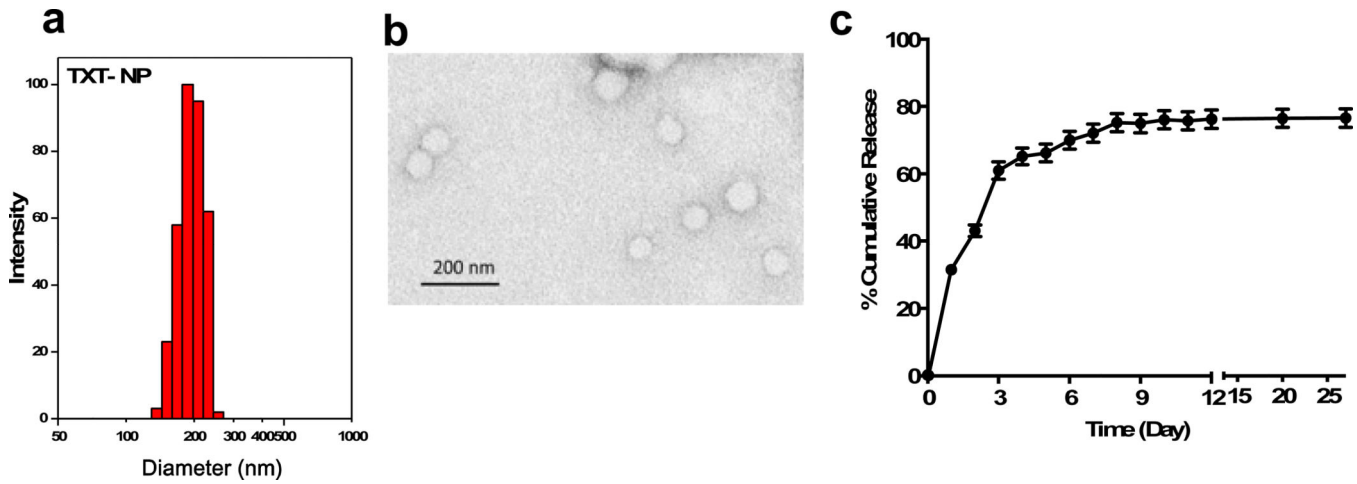

Figure 1: Physical characterization of TXT-NPs and drug release.

a) Histogram showing hydrodynamic size distribution of TXT-NPs measured in water using dynamic light scattering. Mean hydrodynamic diameter = 252 ± 21 nm with polydispersity index of = 0.07, n=7; **b)** Transmission Electron Micrograph (TEM) of TXT-NPs, mean TEM diameter = 60 ± 2.1 nm; n=200; **c)** Drug release profile from TXT-NPs carried out at 37 °C in mannitol citrate buffer pH 7.5 containing 0.1% between 80 and 10% ethanol to maintain sink condition, and 0.1% sodium azide as preservative. Data as mean ± s.e.m., n=3

Author Manuscript Author Manuscript Author Manuscript Author Manuscript

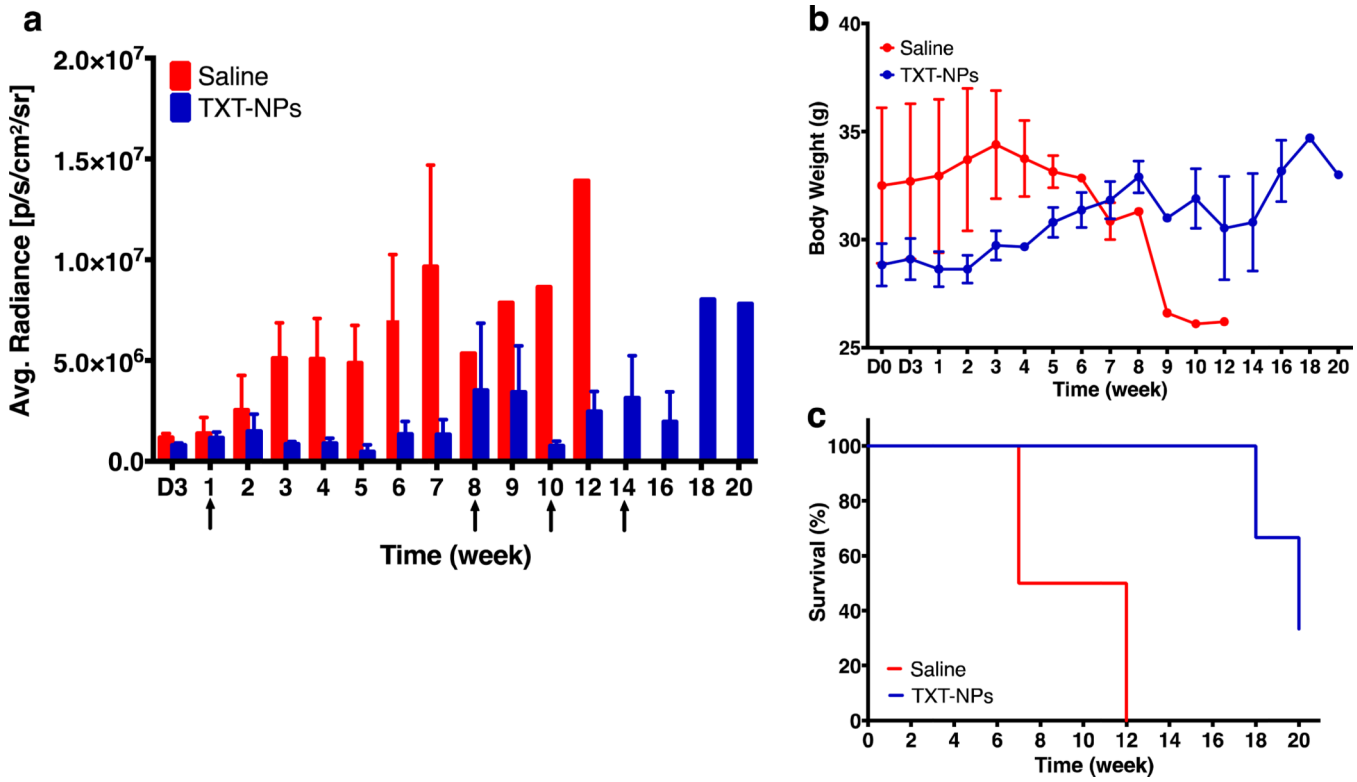

Figure 2: Effect of treatment with TXT-NPs on tumor regression.

Animals were treated with TXT-NPs (12 mg/kg TXT dose equivalent NPs) to determine the effect of first dosing. The subsequent dosing was administered when tumor began to grow. Arrows indicate dosing schedule. Changes in **a)** bioluminance signal in TXT-NPs treated vs. saline control groups, p=0.008; **b)** body weight in treated vs. saline group, p=NS; and **c)** survival of treated vs. saline control, p=0.04. Data are expressed as the mean ± s.e.m., n= 3 to 4. Median survival for saline group = 9.5 wks vs. 20 wks for treated group. X-axis abbreviation: D is for days, whereas other time points are in weeks.

Author Manuscript Author Manuscript Author Manuscript Author Manuscript

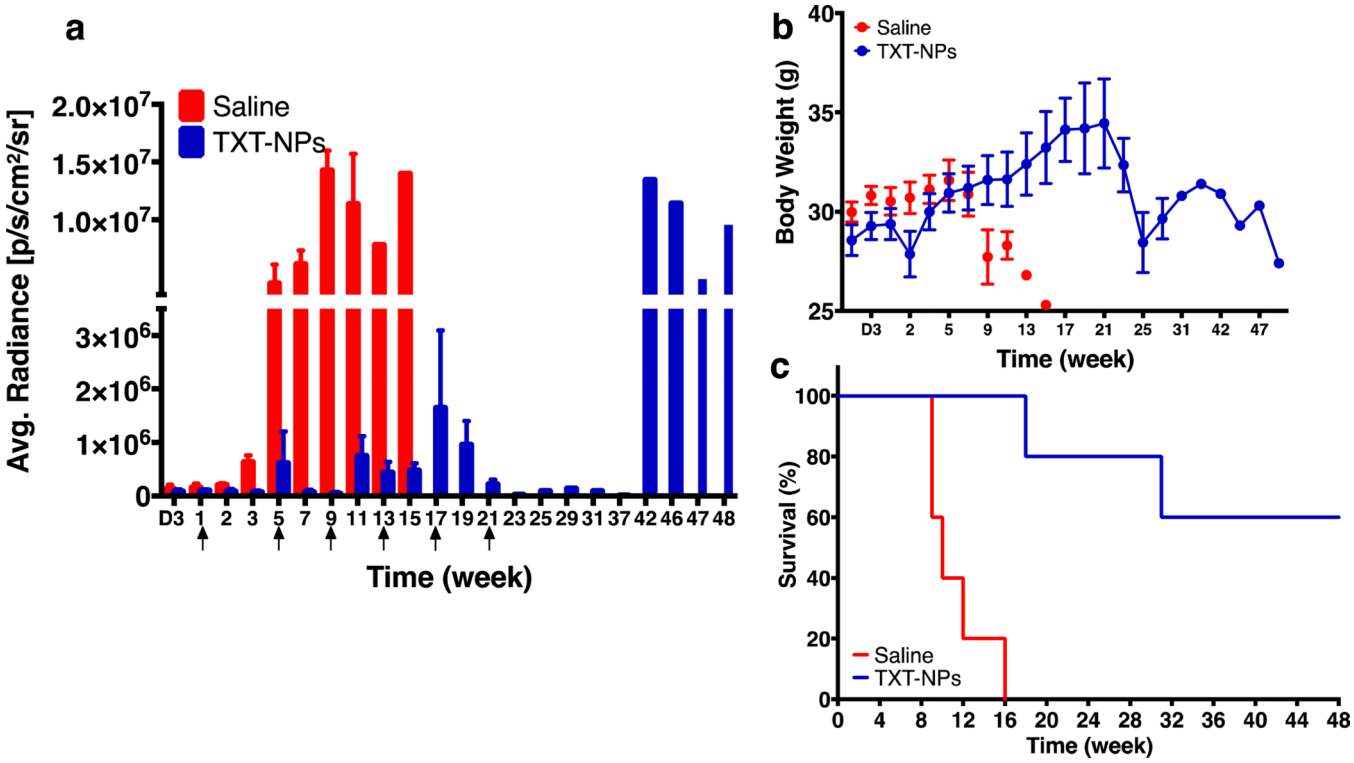

Figure 3: Efficacy of multiple dosing of TXT-NPs at predetermined time points on tumor regression.

Animals were treated with TXT-NPs (12 mg/kg TXT dose equivalent NPs) via tail vein. Arrows indicate dosing schedule, which is at 4 wk-intervals with total six doses. Changes in **a)** bioluminescence signal in TXT-NPs treated and saline control groups; p=0.01 **b)** body weight of treated vs. saline control, p=NS; **c)** survival with time; treated vs. saline p=0.002. Data are expressed as the mean ± s.e.m. n=4 to 5. Median survival for untreated group = 10 wks vs. > 48 wks for the treated group, which is beyond the study end point. Abbreviation, D is for days, whereas other time points are in weeks.

Author Manuscript Author Manuscript Author Manuscript Author Manuscript

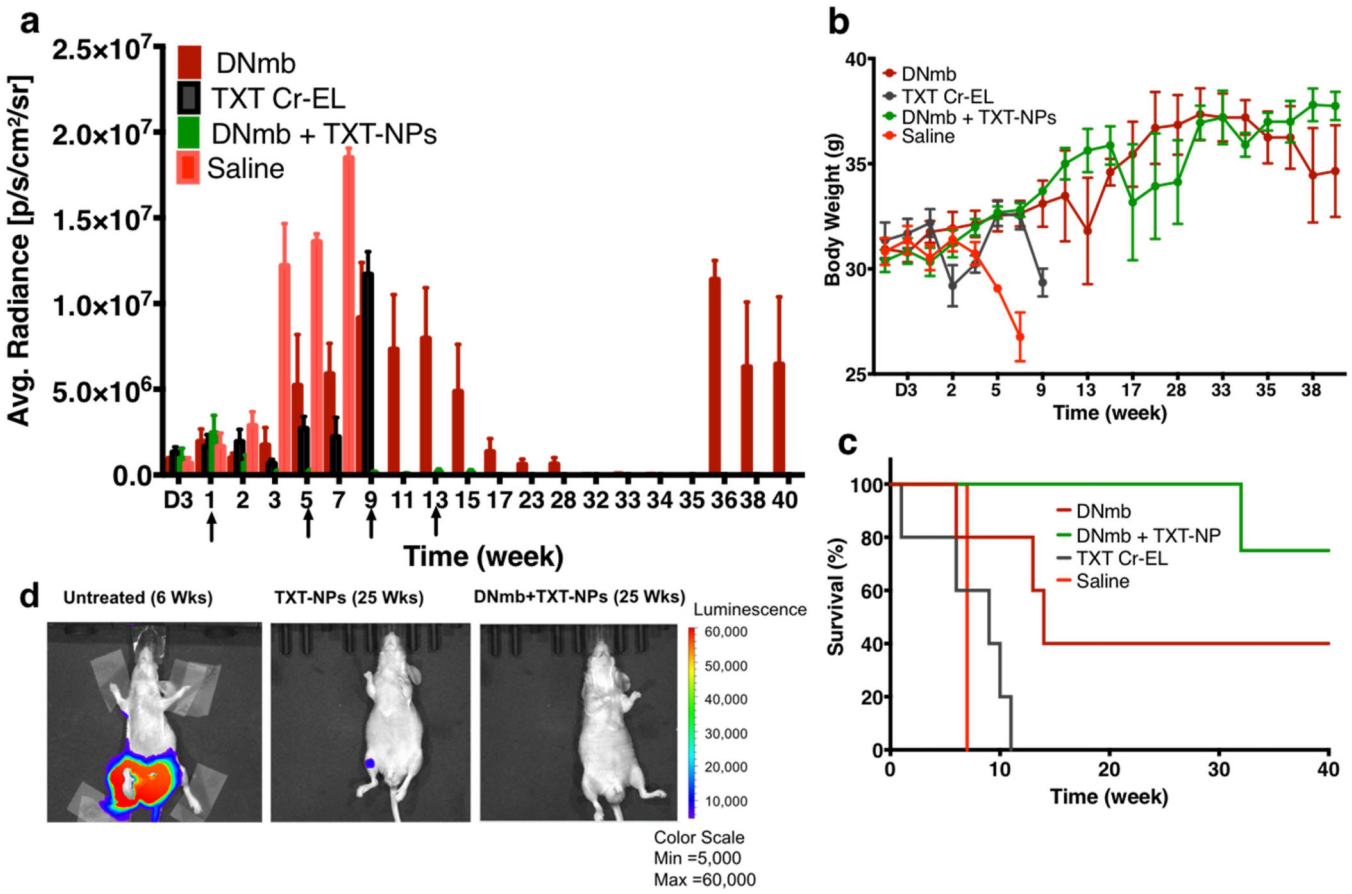

Figure 4: Effect of combination treatment (TXT-NPs + DNmb) on tumor regression.

Animals with tumor received 4 doses of TXT-NPs (12 mg/kg TXT dose-equivalent NPs) in combination with DNmb (3 mg/kg), both given simultaneous as an IV injection. The other groups were DNmb alone (3 mg/kg, as IV injection), TXT-Cremophor (12 mg/kg), and saline (n=3). Arrows indicate dosing schedule. Changes in **a)** bioluminance signal; $p<0.05$ (each group compared with saline group); **b)** body weight, $p<0.05$ for both DNmb and combination treatment when compared with saline control; TXT Cr-EL group shows no statistical significance with saline control; **c)** survival with time; and **d)** representative bioluminance images of untreated, TXT-NPs and the combination (DNmb+TXT-NPs) treated animals. Combination vs. other groups, $p=0.01$. Saline, vs. TXT Cr-EL or DNmb p=NS. Data are expressed as the mean ± s.e.m., n= 3 to 5. The combination treatment was most effective in terms of tumor regression, body weight gain, and survival as compared with other treatment groups. There was no tumor relapse in the combination group even after discontinuing the treatment, whereas DNmb alone treated group showed tumor relapse. Median survival for saline = 7 wks; DNmb =14 wks; TXT-Cr-EL = 9 wks; and DNmb + TXT-NP > 40 wks, which is beyond the study end point. Abbreviation, D is for days, whereas other time points are in weeks.

Author Manuscript Author Manuscript Author Manuscript Author Manuscript

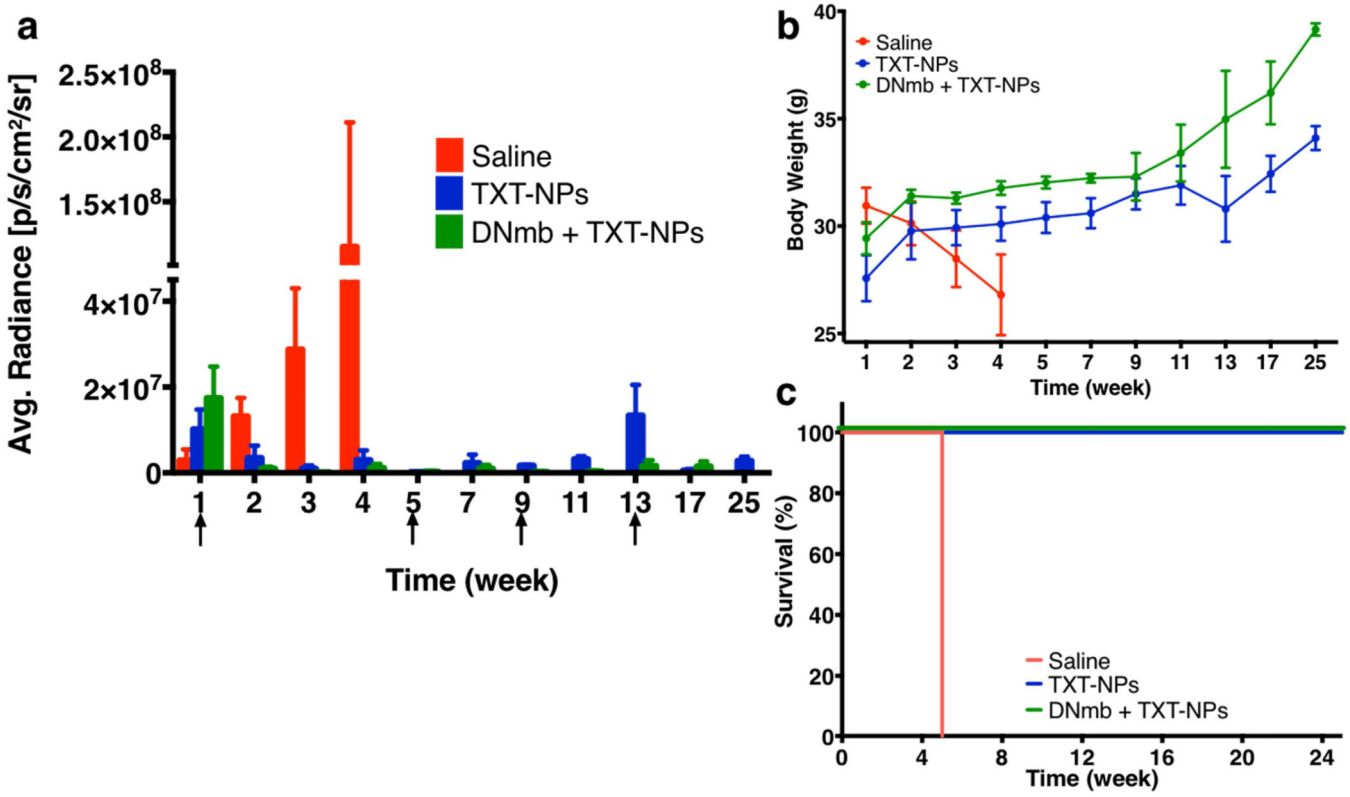

Figure 5: Comparative efficacy of the combination treatment vs. TXT-NPs alone.

Animals with tumor received either DNmb + TXT-NPs (12 mg/kg TXT dose equivalent NPs + 3 mg/kg, DNmb) or TXT-NPs alone (12 mg/kg TXT dose equivalent). Arrows indicate treatment schedule. Changes in **a)** bioluminance signal in treatment groups vs. saline control; $p<0.05$ **b)** body weight, $p= 0.01$ for combination vs. saline group, combination vs. TXT-NPs, p=NS, and **c)** survival with time. Data are expressed as the mean ± s.e.m., n= 3 to 5. Blue (TXT-NPs) and green (combination) lines overlap each other. Treatments vs. saline control $p= 0.001$. Median survival for saline = 5 wks; > TXT-NP or DNmb + TXT-NP > 25 wks, which is beyond the study end point.

Author Manuscript Author Manuscript Author Manuscript Author Manuscript

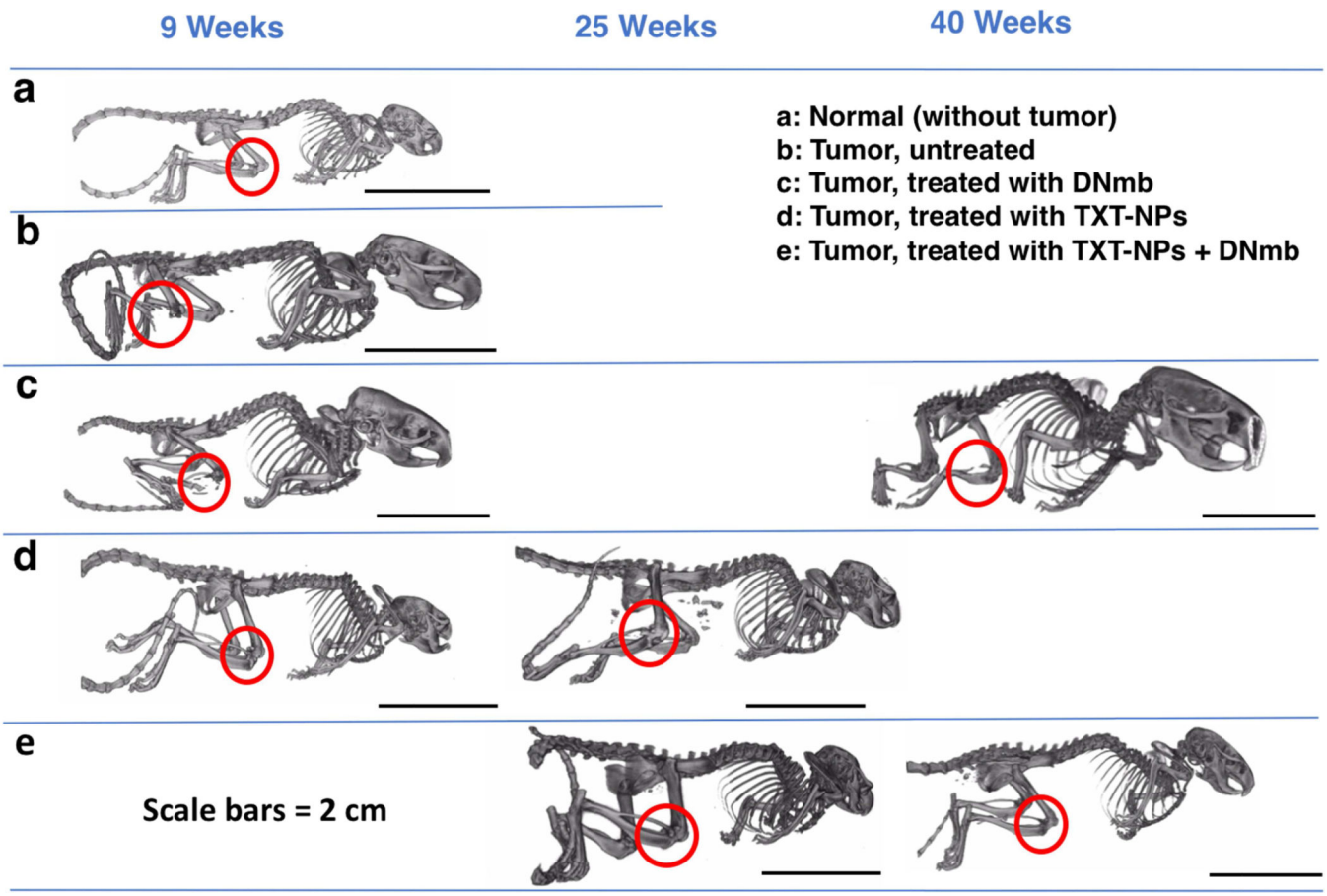

Figure 6: Micro-CT analysis for bone loss.

The micro-CT analysis was carried on representative animals from different treatment groups at 9, 25 and 40 wks. The results show that the combination treatment is most effective in inhibiting bone resorption.

Author Manuscript Author Manuscript Author Manuscript Author Manuscript

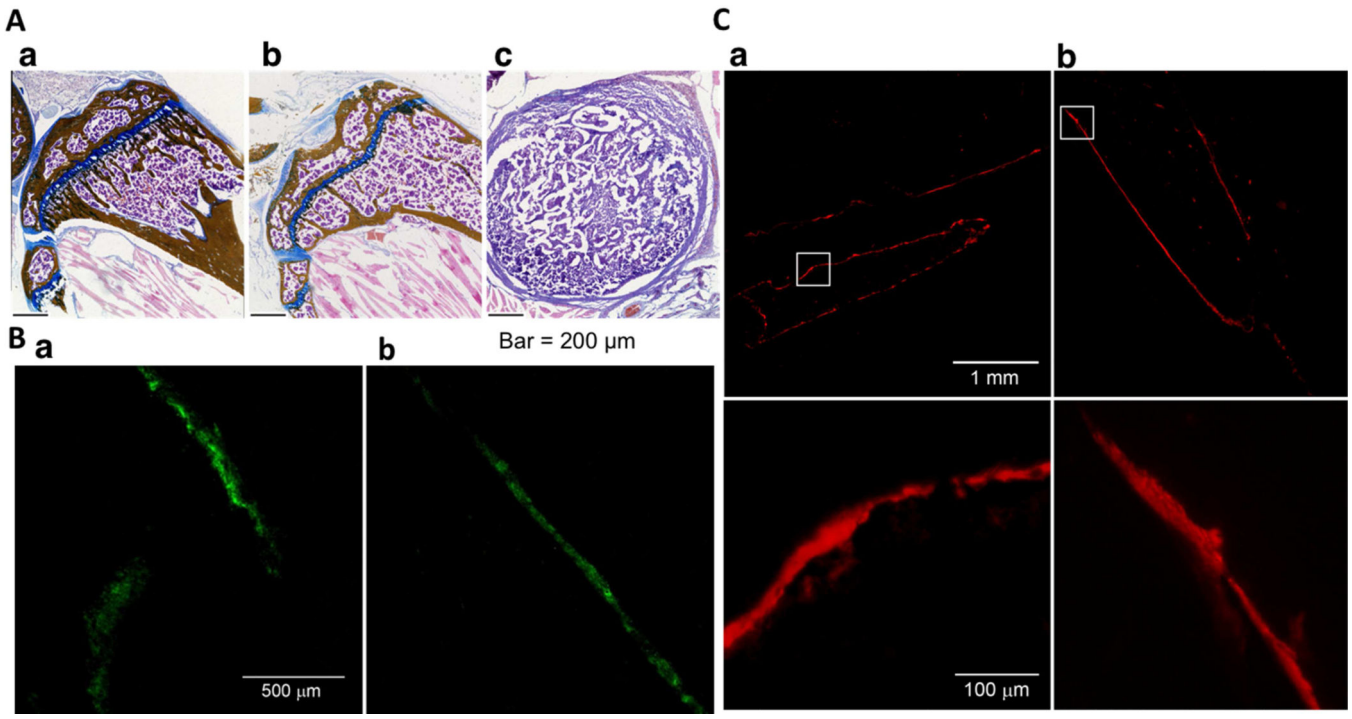

Figure 7: Morphological and immunohistochemical analysis of bone.

A) Histological analysis of bone **a)** normal, **b)** treated with the combination of TXT-NPs + DNmb at 25 wks and **c)** untreated. Treated animal shows almost similar bone morphology as control bone, whereas untreated animal shows only tumor tissue in this region of the tibia. **B)** TRAP staining for osteoclasts of **a)** normal tibia and **b)** tumor-inoculated tibia from the animal treated with the combination of TXT-NPs + DNmb at 25 wks. Tibia from treated animals shows similar osteoclast distribution pattern as tibia from the normal animal (no tumor induction). **C)** Alkaline phosphatase staining for osteoblasts **a)** normal tibia and **b)** tumor-inoculated tibia from the animal treated with the combination of TXT-NPs + DNmb at 25 wks at low and high magnifications. Tibia of the treated animals show normal osteoclast and osteoblast activities.

Author Manuscript Author Manuscript Author Manuscript Author Manuscript

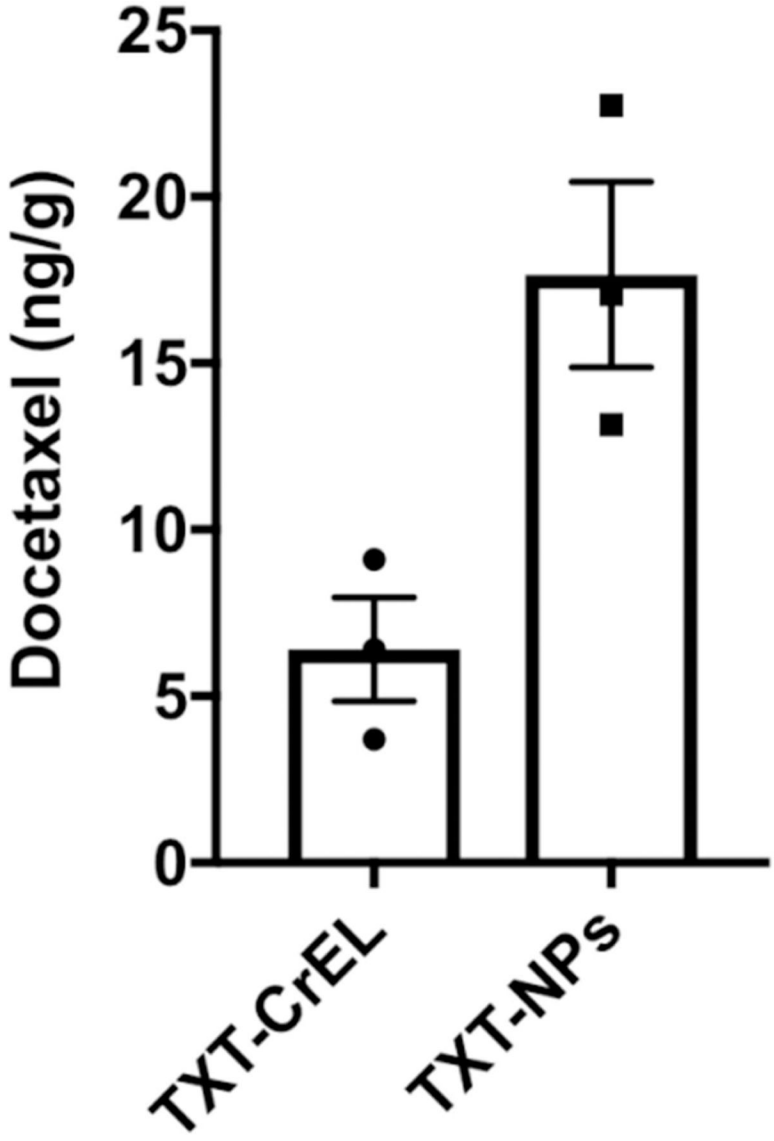

Figure 8: Analysis of TXT levels in metastasized bone tissue.

Animals with tumor signal between 4.98E+06 p/s/cm^2/sr to 1.46E+07 p/s/cm^2/sr range were used. Drug was administered either as TXT-NPs or TXT-CrEL (12 mg/kg) in animals with bone tumor. TXT levels in metastasized bone tissue were analyzed one-week post-drug administration. Results show ~-fold higher drug levels in animals treated with TXT-NPs than with TXT-CrEL. Data as the mean ± s.e.m., n= 3, p=0.02.

Author Manuscript Author Manuscript Author Manuscript Author Manuscript

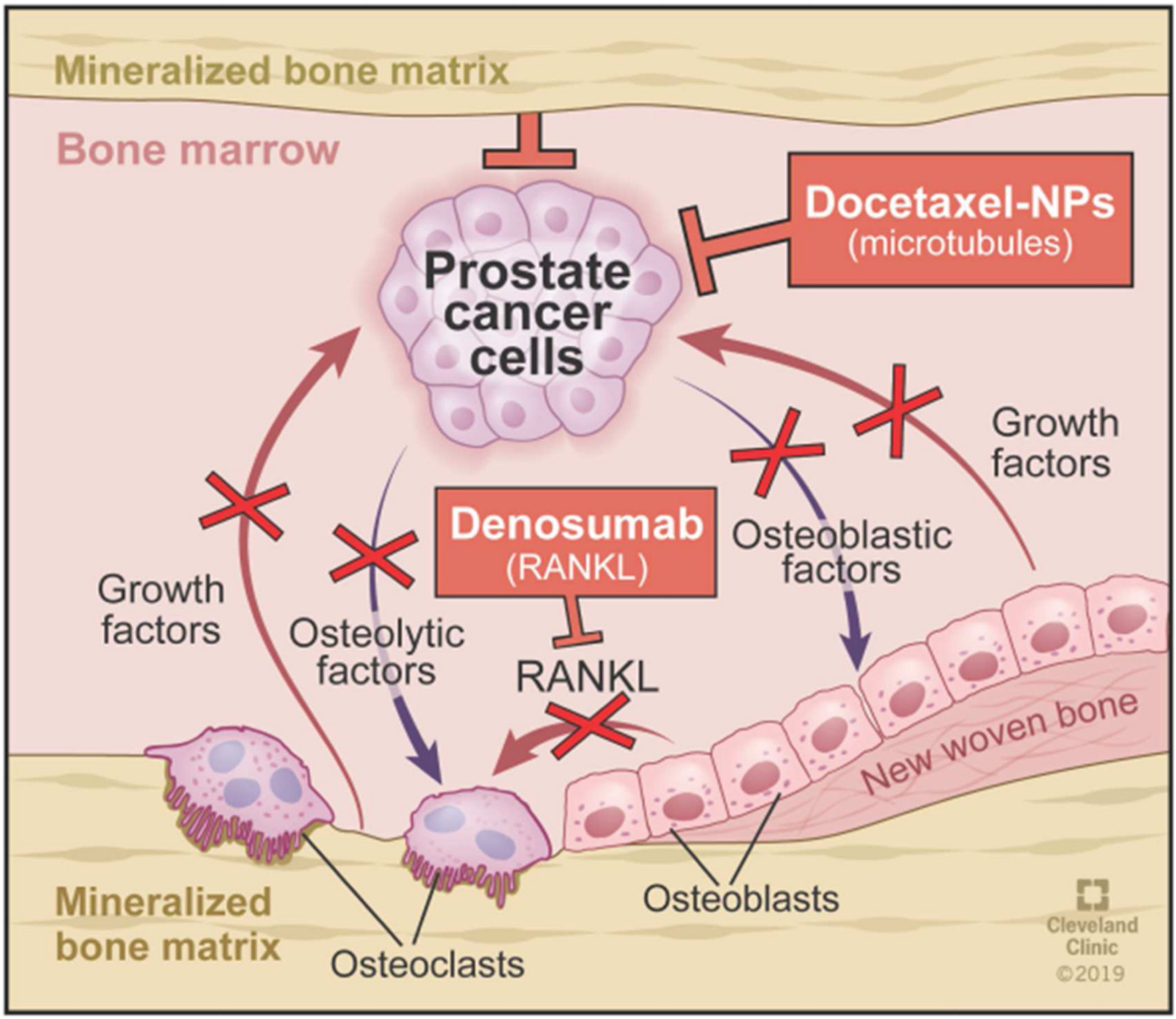

Figure 9: Mechanism of efficacy of the combination of TXT-NPs and DNmb in preventing bone loss.

The combination treatment breaks the communication between prostate cancer cells and osteoclasts that support each other to promote cancer cell growth and osteoblast conversion to osteoclasts.

Author Manuscript

Author Manuscript

Author Manuscript

Author Manuscript

Table 1:

Cytotoxicity of TXT Soln and TXT-NPs in different prostate cancer cell lines

Cell Line	End Point	Treatment	IC_{50} (ng/mL)	IC_{75} (ng/mL)	IC_{90} (ng/mL)
PC3	**3 day**	TXT-Soln	2.5±0.05	4±0.03	6±0.2
		TXT-NPs	2.6±0.04	5±0.1	14±0.3
	5 day	TXT Soln	1.6±0.01	2.5±0.02	5±0.07
		TXT-NPs	2±0.03	4±0.08	15±0.7
	7 day	TXT-Soln	1.6±0.01	2.5±0.01	4±0.08
		TXT-NPs	2±0.01	3.4±0.02	7±0.2
DU145	**5 day**	TXT-Soln	1.5±0.04	2±0.03	2±0.02
		TXT-NPs	1.6±0.03	2.2±0.03	3±0.04
LNCaP	**5 day**	TXT-Soln	8.3±0.3	22±1	60±2
		TXT-NPs	20±0.5	76±3	208±6
C42	**5 day**	TXT-Soln	6±0.2	13±1	34±5
		TXT-NPs	12±0.4	47±3	149±9

Cell seeding density/well/0.1mL in 96-well plate: For 3- and 5-d treatment in PC3 cells – 3,000 cells; for 7-d treatment – 1,500 cells/well. For DU145 cells – 3,000 cells. LNCaP and C42 cells – 10,000 cells. Data represented as mean ± s.e.m. (n=6).

Author Manuscript

Author Manuscript

Author Manuscript

Author Manuscript

Table 2:

Bone analysis using micro-CT from different groups at 25 wks

Treatment	Sample	Bone Mineral Content (mg)	Bone Mineral Density (mg/cc)	Bone Volume Fraction
Control – no tumor, no treatment	Right tibia	17	597	0.7
	Left tibia	16	620	0.7
TXT-NPs	Tumor tibia	15	439	0.5
	Contralateral tibia	15	461	0.5
DNmb + TXT- NP	Tumor tibia	19	483	0.6
	Contralateral tibia	20	465	0.6

Bone Mineral Density (BMD) is BMC (mg)/cubic centimeter of the sample. Bone volume fraction (BVF) is the volume of mineralized bone/unit volume of the sample